Artificial Neural Network Modeling of Thermal and Irradiation Creep Behavior of HT9 Steel

Hongin Kim[a, b], Sunghwan Yeo[a], Jun-Hwan Kim[a], Hyun Woo Seong[a,*], Young-Kook Lee[b]
[a]*Advanced Fuel Technology Development Division, Korea Atomic Energy Research Institute, Daedeok-daero 989-111, Yuseong-gu, Daejeon, 34057, Republic of Korea*
[b]*Department of Materials Science and Engineering, Yonsei University, Seoul, 03722, Republic of Korea*
[*]*Corresponding author: hyunwoo47@kaeri.re.kr*

Keywords : Neutron irradiation, Ferritic/Martensitic Steels (FMS), Nuclear fuel cladding, Creep properties, Machine learning

1. Introduction

HT9 steel is considered a promising candidate material for fuel cladding in Generation IV reactors owing to its excellent mechanical properties and resistance to irradiation-induced swelling [1]. Nuclear fuel cladding serves as the primary barrier against the release of fission products and is therefore a critical structural component governing reactor safety and integrity. Because Generation IV reactors operate at elevated temperatures to achieve high thermal efficiency, the fuel cladding is exposed to high irradiation doses and elevated temperatures. Furthermore, the cladding is subjected to sustained stresses caused by the accumulation of fission gases and fuel swelling; consequently, creep deformation is a major factor determining its long-term structural integrity [2].

Creep is a time-dependent deformation that occurs when a material is subjected to stress at elevated temperatures for an extended period. However, creep testing requires prolonged test durations, and continuous measurement of strain over time under irradiation conditions involves substantial costs and technical challenges. Consequently, creep data for nuclear fuel cladding materials remain limited, making it difficult to obtain sufficient experimental data over a wide range of temperatures, stresses, and irradiation conditions.

In this study, an artificial neural network (ANN) model was developed to predict the creep strain of HT9 steel using thermal creep data obtained at the Korea Atomic Energy Research Institute (KAERI) and irradiation creep data generated in the BOR-60 research reactor [3]. A physics-based loss function was incorporated to ensure physically consistent predictions. The model was validated using independent experimental data and compared with an existing published creep model for HT9 steel.

2. Methods

2.1 ML dataset

A total of 2,790 creep strain data points were collected from published literature and experimental measurements, and their distributions and descriptive statistics are presented in Table 1. To expand the database, data for various 9–12Cr ferritic/martensitic steels (FMS) were included in addition to HT9; however, the predictions and analyses in this study focused on HT9 steel.

The creep dataset consists of sequential measurements acquired over time under identical test conditions. Therefore, assigning data points from the same creep curve to both the training and test sets could result in data leakage. To prevent this, data obtained for the same material, heat-treatment condition, temperature, stress, and irradiation condition were defined as a single experimental group, and the dataset was split at the group level. The model employed 20 input variables representing alloy composition, heat-treatment conditions, test temperature, effective stress, time, and irradiation conditions, while the effective creep strain was used as the output variable. The experimental groups were divided into training, validation, and test sets at a ratio of 8:1:1. The final predictive performance was evaluated on the test dataset using the coefficient of determination (R^2) and root mean square error (RMSE).

2.2 Artificial neural network modeling

Creep strain varies continuously and nonlinearly with time, temperature, and stress. Therefore, a multilayer perceptron-based ANN regression model was employed to generate smooth creep strain curves [4]. Hyperparameters, including the hidden-layer architecture, learning rate, batch size, dropout rate, and weight decay, were optimized through 1,000 Optuna trials [5].

Conventional ANN models may predict negative strains or physically unrealistic trends, particularly in regions with limited data. To suppress such predictions, five physics-based constraint terms were added to the Huber data loss:

$$L_{totla} = L_{Huber} + L_{pos} + L_{time} + L_{stress} + L_{temp} + L_{time-mono}$$

Here, L_{pos} penalizes negative creep strain predictions. The L_{time}, L_{stress}, and L_{temp} terms impose penalties when the predicted strain decreases with increasing time, stress, and temperature,

respectively. $L_{time-mon}$ penalizes cases in which the predicted strain at a later time is lower than that at an earlier time within the same creep test. Because the accumulated dose in dpa also increases with time during irradiation creep, the time-monotonicity constraint accounts for the coupled effects of time and irradiation dose. The final model was validated using the independent test set and external data not used during model development. All computational pipelines were implemented in Python 3.12.

2.3 Model interpretation and comparision

Shapley Additive exPlanations (SHAP) analysis was applied to quantify the contributions of the input variables to the ANN predictions [6]. The most influential input variables were identified using their mean absolute SHAP values, and the effects of temperature, stress, and alloy composition learned by the ANN were examined based on the variation in SHAP values with the corresponding feature values.

Uncertainty was quantified as $\pm 2\sigma$ by performing 500 stochastic forward passes with dropout enabled in the ANN. The HT9 creep behavior predicted by the ANN was also compared with that calculated using the HT9 creep correlation published by Argonne National Laboratory (ANL) [7]. The creep strain was calculated using each model under identical conditions, and the corresponding RMSE values relative to the experimental measurements were compared.

Table 1. Statistical summary of the collected creep dataset.

Variable	Range	Mean ± SD
C (wt%)	0.06–0.21	0.12 ± 0.06
Si (wt%)	0.02–0.38	0.11 ± 0.08
Mn (wt%)	0–1.98	0.45 ± 0.11
Ni (wt%)	0–0.62	0.43 ± 0.13
Cr (wt%)	7.65–12.1	10.13 ± 1.47
Mo (wt%)	0–1.99	0.65 ± 0.31
W (wt%)	0–2.02	1.33 ± 0.74
B (wt%)	0–0.01	0.005 ± 0.01
N (wt%)	0–0.08	0.04 ± 0.03
V (wt%)	0–0.33	0.22 ± 0.06
Nb (wt%)	0–0.18	0.09 ± 0.08
Ta (wt%)	0–0.12	0.03 ± 0.03
Normalizing temp (°C)	980–1100	1040.41 ± 15.23
Normalizing time (min)	2–60	7.57 ± 7.33
Tempering temp (°C)	650–780	756.48 ± 20.25
Tempering time (min)	30–150	48.42 ± 27.69
Test temp (°C)	300–680	587.16 ± 81.83
Effective stress (MPa)	3.64–333.42	54.66 ± 44.83
Time (h)	0–50925.93	10097.4 ± 8227.94
Dose (dpa)	0–207	13.42 ± 31.16
Effective strain (%)	0–7.59	0.5 ± 0.74

3. Results and Discussion

Hyperparameter optimization is an essential step in improving the predictive performance and interpretability of machine learning models. Fig. 1(a) shows the variation in the objective function over 1,000 trials performed using Optuna. The objective function decreased rapidly during the initial trials and then gradually converged, reaching its minimum value at trial 906. Accordingly, the final model was trained using the optimal hyperparameters obtained from this trial. Fig. 1(b) compares the predicted and measured effective strains for the test dataset. The optimized model achieved an RMSE of 0.311% and an R^2 of 0.887. Most predictions were distributed close to the ideal prediction line, demonstrating that the developed model accurately predicted the effective strain across the test dataset.

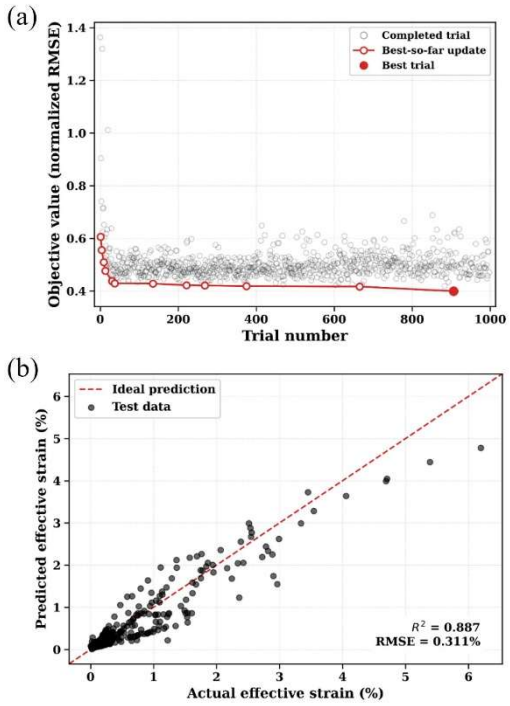


Fig. 1. Optimization of the ANN model: (a) object function values across Optuna trials and (b) prediction of the optimized ANN model for the test dataset.

In addition to the test dataset, independent experimental data not used for model training were employed to further evaluate the generalization performance of the ANN model. Fig. 2 compares the measured and predicted effective strains as a function of time under (a) thermal creep and (b) irradiation creep conditions. For thermal creep, the ANN model achieved an RMSE of 0.096% and successfully reproduced the overall increase in creep strain with time, showing reasonable agreement with the experimental measurements even in the long-term regime. For irradiation creep, only one experimental data point is presented because of the limited availability of experimental data. Despite the limited validation data, the experimental point was located within the model's prediction range, and the model reasonably predicted the

increasing trend in creep strain with time. These results demonstrate the potential of the developed ANN model to represent both thermal and irradiation creep behavior and to predict long-term creep deformation.

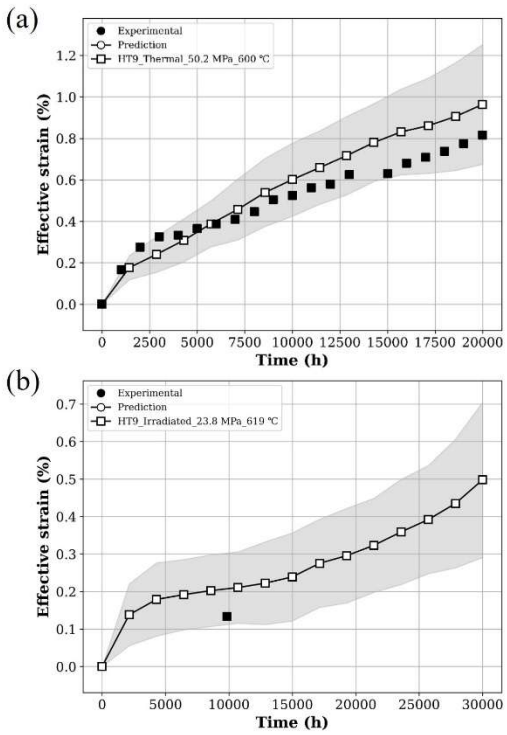


Fig. 2. Validation of the ANN model using data excluded from training: (a) thermal creep of HT9 at 600 ℃ and 50.2 MPa effective stress and (b) irradiation creep of HT9 at 619 ℃, 23.8 MPa effective stress, and 16.8 dpa.

Fig. 3 presents the SHAP analysis performed on all samples, illustrating the relative influence of each input variable on the model's effective strain predictions. Test temperature, effective stress, time, and dose (dpa), which are directly related to the creep test conditions, exhibited the highest feature importance, with test temperature being the most influential variable. Among the alloying elements, Si, Nb, Ni, C, N, W, and V were identified as important variables, although their SHAP importance values were relatively similar. Nb, V, C, and N are the principal elements involved in the formation of fine MX carbonitrides in FMSs. Their inclusion among the highly ranked variables suggests that MX precipitates may be closely associated with creep deformation behavior. In addition, W is known to contribute to solid-solution strengthening by dissolving in the matrix, thereby improving creep resistance, and was also ranked among the 12 most influential variables in the present analysis [8].

Fig. 4 compares the HT9 irradiation creep strain predicted using the correlation reported by ANL and the ANN model developed in this study with independent irradiation creep data obtained from the BOR-60 reactor [3]. The RMSE values for the two validation points were 0.12% and 0.06% for the ANL correlation and ANN model, respectively. Thus, the ANN model reduced the RMSE by approximately 50% relative to the ANL correlation, demonstrating improved predictive performance for the independent experimental data.

In addition to its predictive accuracy, the ANN model reasonably reproduced the time-dependent irradiation creep behavior. Below approximately 5,000 h, the model exhibited primary creep behavior, characterized by a gradual decrease in the creep strain rate. This was followed by secondary steady-state creep, during which the strain increased at a relatively constant rate with time. Under both irradiation conditions, the ANN predictions agreed well with the validation data and appropriately represented the long-term increase in creep strain. In contrast, the ANL correlation tended to overestimate or underestimate the steady-state creep rate depending on the test conditions. At 619 ℃ and 23.8 MPa, it overestimated both the creep strain and steady-state creep rate, whereas at 651 ℃ and 3.6 MPa, it underestimated them. These results suggest that the ANN model can more effectively predict irradiation creep behavior than the conventional empirical correlation by accounting for the combined effects of temperature, stress, irradiation dose (dpa), and time.

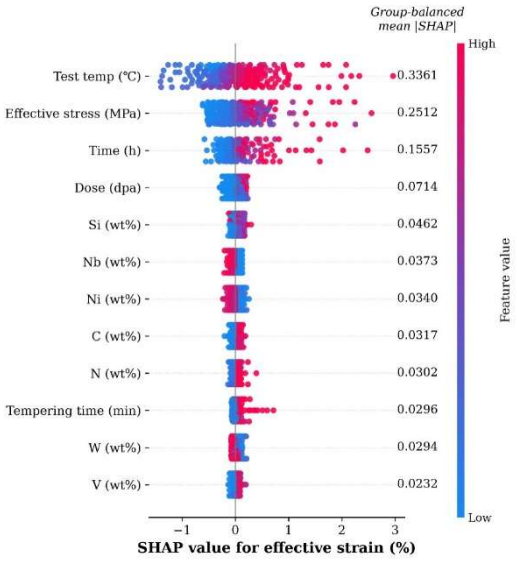


Fig. 3. SHAP summary (beeswarm) plots showing the top 12 variables influencing creep strain (%).

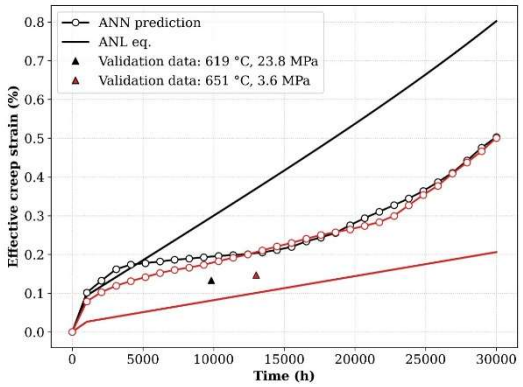


Fig. 4. Irradiation creep strain predicted by the ANN model and ANL creep equation.

4. Conclusion

In this study, an ANN model was developed to predict the thermal and irradiation creep strains of HT9 steel. The model optimized using Optuna achieved an RMSE of 0.311% and an R^2 of 0.887 on the test dataset. It also reasonably reproduced the time-dependent creep strain and primary and secondary steady-state creep behavior observed in independent experimental data. SHAP analysis identified test temperature, effective stress, time, and irradiation dose (dpa) as the most influential predictors, while alloying elements such as Nb, V, C, N, and W also exhibited notable contributions to the predicted creep behavior. In comparison with the BOR-60 irradiation creep data, the ANN model achieved an RMSE of 0.06%, reducing the error by approximately 50% relative to the RMSE of 0.12% obtained using the ANL correlation. The ANN model also mitigated the overestimation or underestimation of the steady-state irradiation creep rate under different test conditions. These results demonstrate that the developed ANN model can effectively predict thermal and irradiation creep behavior by accounting for the combined effects of test conditions and alloy composition.

REFERENCES

[1] D.-H. Kim, C.M. Lee, J.-H. Kim, S.-H. Kim, S. Yeo, Y.-K. Lee, Thermal creep analysis and correlation development for manufactured HT9 cladding, Journal of Nuclear Materials 593 (2024) 154999.
[2] E.H. Jeong, J.H. Kim, S.H. Kim, Y.D. Kim, Effect of boron on the thermal stability of the precipitate phase of FC92B and FC92N steels during aging and creep, Metals and Materials International 27(5) (2021) 985-994.
[3] S.H. Kim, J.H. Kim, S.G. Park, S.H. Shin, W.S. Ryu, Fabrication and evaluation of advanced cladding tube for PGSFR, International Conference on Fast Reactors and Related Fuel Cycles: Next Generation Nuclear Systems for Sustainable Development (FR17), International Atomic Energy Agency, Yekaterinburg, Russian Federation, 2018.
[4] G. James, D. Witten, T. Hastie, R. Tibshirani, An Introduction to Statistical Learning, Springer, New York, 2013.
[5] T. Akiba, S. Sano, T. Yanase, T. Ohta, M. Koyama, Optuna: A next-generation hyperparameter optimization framework, Proceedings of the 25th ACM SIGKDD International Conference on Knowledge Discovery & Data Mining, Association for Computing Machinery, Anchorage, Alaska, USA, 2019, pp. 2623-2631.
[6] A.E. Roth, The Shapley Value: Essays in Honor of Lloyd S. Shapley, Cambridge University Press, Cambridge, 1988.
[7] L.L. Briggs, L.K. Chang, D.J. Hill, Safety Analysis and Technical Basis for Establishing an Interim Burnup Limit for Mark-V and Mark-VA Fueled Subassemblies in EBR-II, ANL-NSE-1, Argonne National Laboratory, 2018.
[8] T. Sakthivel, K. Laha, P. Parameswaran, S. Panneer Selvi, K. Chandravathi, M. Mathew, Effect of thermal aging on microstructure and mechanical properties of P92 steel, Transactions of the Indian Institute of Metals 68(3) (2015) 411-421.